Chinese Chemical Letters 35 (2024) 110274

Contents lists available at ScienceDirect

Chinese Chemical Letters

journal homepage: www.elsevier.com/locate/cclet

Assembly of Y(III)-containing antimonotungstates induced by malic acid with catalytic activity for the synthesis of imidazoles

Guoping Yang[a,b,1,*], Zhoufu Lin[a,1], Xize Zhang[a], Jiawei Cao[a], Xuejiao Chen[a], Yufeng Liu[a,b], Xiaoling Lin[a,*], Ke Li[a,*]

[a] School of Nuclear Science and Engineering, Jiangxi Key Laboratory for Mass Spectrometry and Instrumentation, Jiangxi Province Key Laboratory of Functional Organic Polymers, East China University of Technology, Nanchang 330013, China
[b] College of Chemistry, Xinjiang University, Urumqi 830017, China

ARTICLE INFO

Article history:
Received 10 July 2024
Revised 15 July 2024
Accepted 16 July 2024
Available online 16 July 2024

Keywords:
Polyoxometalates
Yttrium
Antimonotungstate
Malic acid
Imidazoles

ABSTRACT

A dimeric Y(III)-containing antimonotungstate $[Y_4(H_2O)_8(mal)_2(OAc)O(Sb_2W^{V}_2W^{VI}_{19}O_{72})_2]^{21-}$ (**Y_4mal_2**, H_3mal = DL-malic acid), resembling a "handshake" configuration, was synthesized and characterized. The polyanion of **Y_4mal_2** consists of two Dawson-derived $\{Y_2Sb_2W_{21}\}$ moieties that are further linked by two mal ligands and one μ_2-bridging acetate to form an asymmetric polyanion. Notably, the chiral configuration induced by the D- or L-configuration of the mal ligand results in both $\{Y_2Sb_2W_{21}\}$ moieties within one polyanion exhibiting identical chirality, leading to the racemate crystallization of **Y_4mal_2**. Moreover, **Y_4mal_2** exhibits excellent Lewis acid catalytic activity for environmentally friendly synthesis of imidazoles.

The study of polyoxometalates (POMs) commenced in 1826 and has since experienced rapid development [1,2]. Benefiting from the fascinating structural diversity and designability, POMs continue to garner great attention not only in the field of crystallography and cluster science but also in catalysis, luminescence, optics, magnetics, and medicine applications [3-13]. The synthetic chemistry of POMs remains fundamental for discovering functional applications that contribute to the long-term advancement of POMs chemistry [14]. Transition metals (TMs), especially rare earth metals (REs), exhibiting multiple coordination modes and diverse properties associated with their atomic structures, can act as "inorganic functional groups" when participating in the assembly of POMs to synthesize TM- or RE-encapsulated POMs [15-21]. The well-developed TM- and RE-encapsulated POMs can be valuable models for bridging microscopic metal-oxo-clusters with macroscopic physical and chemical properties [22-25]. However, there are still challenges for the synthesis of RE-encapsulated POMs. Generally, oxytropic RE ions tend to rapidly hydrolysis or combine with oxygen-rich building units within POMs assemblies, leading to the formation of amorphous precipitates. To address this issue, the most popular approach is utilizing oxygen-containing organic ligands. Among these options, malic acid stands out as a representative ligand due to its various coordination modes.

To the best of our knowledge, there are only limited cases of mal-functionalized RE-encapsulated POMs since the first enantiomers $[(\alpha\text{-}P_2W_{16}O_{59})Zr_2(\mu_3\text{-}O)(D\text{-}/L\text{-}mal)]_2^{18-}$ reported by Hill in 2005 [26]. They are $[M(L\text{-}mal)P_2W_{17}O_{61}]^{8-}$ (M = Zr and Hf) reported by Sokolov in 2009 [27], $[Ln_3(\mu_3\text{-}OH)(H_2O)_8(AsW_9O_{33})(AsW_{10}O_{35}(mal))]_2^{22-}$ (Ln = Dy, Tb, Gd, Eu, and Sm) reported by Niu's group in 2015 [28], $\{Ce_3(H_2O)_9[As_2W_{21}O_{72}(mal)_2]\}^{9-}$ reported in 2017 [29], $[\{Pr(H_2O)_2\}_2\{As_2W_{19}O_{68}\}\{WO_2(mal)\}_2]^{12-}$ reported in 2018 [30], enantiomeric $[Zr_4(\mu_3\text{-}O)_2(D\text{-}/L\text{-}mal)_2(B\text{-}\alpha\text{-}HSiW_{10}O_{37})_2]^{8-}$, enantiomeric $[Zr_4(\mu_3\text{-}O)_2(D\text{-}/L\text{-}mal)_2(B\text{-}\alpha\text{-}PW_{10}O_{37})_2]^{8-}$ reported by Zhao and Yang in 2019 [31], $[RE_3(\mu_3\text{-}OH)(H_2O)_8(AsW_9O_{33})(AsW_{10}O_{35}(DL\text{-}mal))]_2^{22-}$ (RE = Er, Y, and $Er_{0.05}Y_{0.95}$) reported by Niu in 2020 [32], $[Ln_4(H_2O)_{14}W_7O_{15}(H_2mal)_4][Sb^{III}W_9O_{33}]_2[HP^{III}Sb^{III}W_{15}O_{54}]_2^{20-}$ (Ln = Nd and Pr) reported by Wang and Zhao in 2022 [33], and $[Ln_4(H_2O)_{14}W_6O_{13}(OH)_5(mal)_2(B\text{-}\alpha\text{-}TeW_9O_{33})_4]^{19-}$ (Ln = La, Ce, and Pr) reported by Ma and Niu's group in 2024 [34] and so on. Furthermore, the addition of malic acid during the synthesis process is still essential for the formation of some specific structures, even if mal ligands did not join in the coordination. Examples are $[(DyOH_2)_3(CO_3)(\alpha\text{-}PW_9O_{34})_2]^{11-}$ [35], $[Cu(im)_4][Na_2Cu_3(H_2O)_3Cu(H_2O)_2(SbW_9O_{33})_2]^{6-}$ [36], $[H_2(Sb^{III}W^{VI}_9O_{33})(W_5O_{12})(Sb^{III}_2W^{VI}_{29}O_{103})]^{27-}$ [37] and so on.

* Corresponding authors.
E-mail addresses: erick@ecut.edu.cn (G. Yang), xiaoling@ecut.edu.cn (X. Lin), like@ecut.edu.cn (K. Li).
[1] These authors contributed equally to this work.

https://doi.org/10.1016/j.cclet.2024.110274
1001-8417/

It is evident from the documented structures that nearly all of these polyanions exhibit centrosymmetric configurations, including the rarely reported chiral enantiomers. The distinctive asymmetric structure of malic acid offers an advantage in creating novel asymmetric architectures with unique properties; however, these structures are seldom explored.

In this study, we present a rare racemic Y(III)-containing antimonotungstate dimer, $[Y_4(H_2O)_{10}(mal)_2(OAc)O(Sb_2W^{V}{}_2W^{VI}{}_{19}O_{72})_2]^{21-}$ (**Y_4mal_2**), which exhibits an intriguing handshake-like configuration. Additionally, Y_4mal_2 demonstrates remarkable catalytic activity and reusability in the synthesis of 2,4,5-trisubstituted imidazoles *via* cyclocondensation reactions involving benzil, aldehyde, and ammonium acetate. The yields of imidazoles are up to 98% and **Y_4mal_2** can be reused at least 5 times without significant deactivation, revealing its potential for practical application.

Single-crystal analysis reveals that **Y_4mal_2** crystallizes in the $P2_1/c$ space group from the monoclinic crystal system (Table S1 in Supporting information). The asymmetric unit based on the SQUEEZE-treated data consists of one asymmetric $[Y_4(H_2O)_{10}(mal)_2(OAc)O(Sb_2W^{V}{}_2W^{VI}{}_{19}O_{72})_2]^{25-}$ polyanion, eight disordered Na^+ ions (4 occupancies in total), and four water molecules coordinated with Na^+ ions (2 occupancies in total). The polyanion of **Y_4mal_2** exhibits a unique asymmetric configuration that two Dawson-like $\{Y_2(Sb_2W_{21})\}$ moieties are linked by mal ligands and μ_2-acetate with a rotation at the vertex-sharing O13 (Figs. 1, 2a and 2b). This Dawson-like $\{Y_2(Sb_2W_{21})\}$ moieties may be treated as a derivative of typical $\{X_2W_{21}\}$ moieties in which two Y(III) ions are inserted into the sandwich part. Alternately, the polyanion of **Y_4mal_2** can also be divided into five parts from the standpoint of structure decomposition, including one $\{Y_4W_4(W_2)(mal)_2(OAc)\}$ cluster and four $\{B\text{-}\alpha\text{-}SbW_9O_{33}\}$. Four $\{B\text{-}\alpha\text{-}SbW_9O_{33}\}$ are connected with the $\{Y_4W_4(W_2)(mal)_2(OAc)\}$ cluster *via* W-O-W and W-O-Y bonds to form the complete polyanion. It should note that the four of the six $\{WO_6\}$ octahedrons (W11/W21/W32/W42) in the $\{Y_4W_4(W_2)(mal)_2(OAc)\}$ cluster are isolated with each other, while the μ_2-acetate-linked two $\{WO_6\}$ (W1/W22) are vertex-sharing *via* O13. Four Y(III) ions and six $\{WO_6\}$ octahedrons share vertex-oxygen atoms to form the almost centrosymmetric $\{Y_4W_4(W_2)(mal)_2(OAc)\}$ cluster together with the coordination of mal ligands.

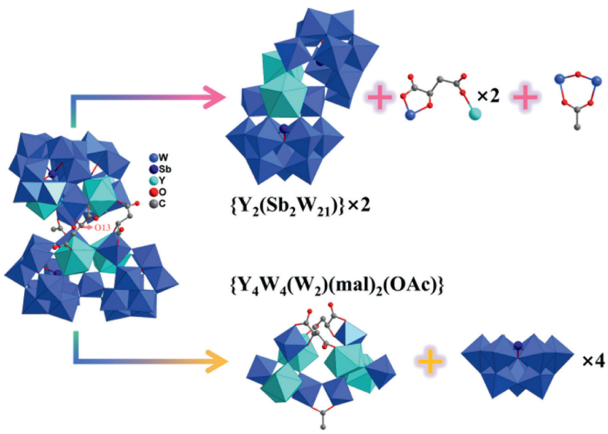

Fig. 1. View of the two routes for the structure decomposition of the polyanion in Y_4mal_2. Top, two Dawson-like $\{Y_2(Sb_2W_{21})\}$ moieties, two mal ligand, and one μ_2-bridging acetate; Bottom, $\{Y_4W_4(W_2)(mal)_2(OAc)\}$ moieties and four $\{B\text{-}\alpha\text{-}SbW_9\}$ moieties.

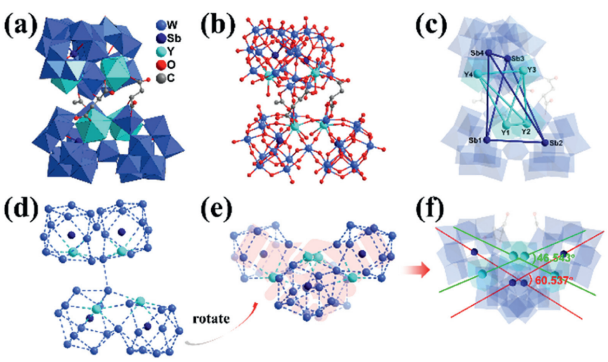

Fig. 2. (a) Polyhedral and (b) ball-and-stick view of the polyanion of **Y_4mal_2**. (c) View of the spatial distribution of Y1-Y4 and Sb1-Sb4 atoms in one polyanion. (d) View of the simplified diagram of the polyanion. (e) Top view of the handshake-like configuration. (f) Top view of the rotation of two $\{Y_2(Sb_2W_{21})\}$ moieties.

The four crystallographically independent Y(III) ions in **Y_4mal_2** exhibit similar 8-coordinated geometries (Fig. S1 in Supporting information). Y1 and Y3 are both coordinated with two water molecules and six oxygen atoms provided by $\{Sb_2W_{21}\}$ moieties. For comparison, Y2 and Y4 are coordinated with three water molecules and five oxygen atoms from $\{Sb_2W_{21}\}$ moieties. The bond lengths of Y-O bonds are in the range of 2.20–2.47(2) Å. Furthermore, we respectively connected four Y(III) ions and four Sb(III) atoms to form two interpenetrating distorted tetrahedrons. The distances of Y1 and Y2, Y3 and Y4, Sb1 and Sb2, Sb3 and Sb4 are 5.7987, 5.8102, 7.1895, and 7.1904 Å, respectively (Fig. 2c). To simplify the polyanion, all the nonmetallic atoms are omitted to obtain the simplified diagrams of the polyanion, which represent a handshake-like configuration from the top view (Figs. 2d and e). The projection of the polyanion from the top view shows a nearly centrosymmetric configuration and the lines of Sb1-Sb2 and Sb3-Sb4 have a space angle of 60.537°, while the space angle between the lines of Y1-Y2 and Y3-Y4 is only 46.543° (Fig. 2f). Obviously, the Sb-lines and Y-lines are not parallel. By comparison, the space angle of Sb-lines can better reflect the degree of the rotation of two $\{(Y_2Sb_2W_{21})\}$ moieties and the asymmetry of polyanion.

The two mal ligands show almost the same μ_3-bridging coordination mode that one oxygen atom from the carboxyl and the α-OH cheat with one W(VI) atom to form a $\{WO_6\}$ octahedron (Fig. S2 in Supporting information). The other carboxyl group exhibits a trans-μ_2-bridging mode with one disordered Na^+ ion and one Y(III) ion. It should be noted that the mal ligands in Figs. 1 and 2 are all in their D-configuration and the $\{Y_2(Sb_2W_{21})\}$ moieties are also "right-oblique". The angles of inclination are about 62.921° for Sb1Sb2-$\{Y_2(Sb_2W_{21})\}$ and 62.655° for Sb3Sb4-$\{Y_2(Sb_2W_{21})\}$, respectively (Fig. S3 in Supporting information). This phenomenon means that the single polyanion of **Y_4mal_2** is monochiral. However, **Y_4mal_2** only crystallized in the achiral space group. Based on the usage of DL-mal ligand in the synthetic procedure and the analysis of spatial structure, **Y_4mal_2** is racemic and two kinds of enantiomeric polyanions are 1:1 crystallized (Fig. S4 in Supporting information).

Based on the above-mentioned structural analysis, we can find the fact that the coordination environments of Y1/Y3 and Y2/Y4, two $\{Y_2(Sb_2W_{21})\}$ moieties, and two mal ligands are all very similar and the projection of the polyanion exhibits a nearly centrosymmetric configuration. However, the asymmetric polyanion of **Y_4mal_2** did not crystallize based on the symmetry of the higher symmetric space group such as $C2/c$. The disordered parts (such as Na^+ ions coordinated with the polyanion) in the asymmetric unit may be responsible for this phenomenon.

The formula of **Y_4mal_2** was determined by the combination of single-crystal data, ICP-OES, EA, and TGA results. The origin single-crystal data without the treatment of SQUEEZE gave approximate numbers of Na^+ and $(CH_3)_2NH_2$ cations of about 13 and 8, which are further verified by ICP-OES and EA results. ICP-OES result gave the mass fractions of 1.49%, 2.80%, and

60.60% for Na, Y, and W, respectively. Thus, the molar ratio of Na:Y:W in **Y_4mal$_2$** is about 13:4:42. The mass fraction ratio of C:H:N = 2.13:0.99:0.90 was obtained from the EA result. Thus, the number of $(CH_3)_2NH_2$ cations removed in the SQUEEZE process is about 8. The valences of Y and Sb atoms are all determined as +3 based on the BVS results (Table S2 in Supporting information), W6, W21, W37, and W39 are pentavalent, and other W atoms are hexavalent. Besides, a weight loss of 6.79% at 129 °C was found based on the TGA curve which corresponds to approximately 48 water molecules (Fig. S6 in Supporting information). Therefore, the formula for **Y_4mal$_2$** can be represented as $((CH_3)_2NH_2)_8Na_{13}H_4[Y_4(H_2O)_{10}(mal)_2(OAc)O(Sb_2W^V_2W^{VI}_{19}O_{72})_2]\cdot 38H_2O$. Other texts including FT-IR spectra, PXRD, and solid-state UV diffuse reflection spectrum are shown in Figs. S5, S7 and S8 (Supporting information).

Imidazoles, as a kind of classical heterocyclic structures, have extensive applications in the fields of biomedicine, materials science, and organic synthesis [38-40]. The condensation of aldehydes, benzil, and ammonium acetate catalyzed by acid catalysts represents the most direct and efficient strategy for the construction of imidazoles. Various catalytic systems have been reported based on this cyclocondensation strategy [41-47]. However, these systems still suffer from drawbacks such as environmental pollution caused by metal catalysts and organic solvents, as well as harsh reaction conditions and so on. It is worth noting that the Lewis acid nature of RE endows RE-POMs remarkable Lewis acid catalytic activity. Drawing upon our experiences in POMs-catalyzed the construction of heterocyclic compounds [4,7,48-52], we believe that the cyclocondensation of aldehydes, benzil, and ammonium acetate catalyzed by **Y_4mal$_2$** for imidazole synthesis is anticipated.

Initially, the reaction of benzil (**1a**, 0.2 mmol), benzaldehyde (**2a**, 0.2 mmol), and ammonium acetate (**3a**, 0.6 mmol) was employed to elucidate the catalytic performance of **Y_4mal$_2$**. Delightedly, in the presence of **Y_4mal$_2$** under solvent-free conditions at 100 °C for 2 h, the desired imidazole **4a** was obtained with a 69% yield, which is much higher than the blank experiment (Table 1, entries 1 and 2). Subsequently, a series of green solvents such as dimethyl carbonate (DMC), propylene carbonate (PC), H_2O, and EtOH was added to the reaction mixture to investigate the effect of the solvent. Most solvents are less effective than solvent-free conditions, but the yield increased to 92% using ethanol as solvent (Table 1, entries 3–6). The transformation was sensitive to the reaction temperature, when the temperature was 90 °C, the yield decreased from 92% to 80%, and at 110 °C, the yield reached 98% (Table 1, entries 7 and 8). The reaction was unaffected by increasing the reaction time to 2.5 h, but a shorter reaction time (1.5 h) resulted in a lower yield. A better result was not obtained by changing the catalyst loading, so the optimal catalytic condition was: **1a** (0.2 mmol), **2a** (0.2 mmol), **3a** (0.6 mmol), **Y_4mal$_2$** (0.5 mol%), EtOH (1 mL) under 110 °C for 2 h.

Table 1
Optimization of reaction conditions.[a]

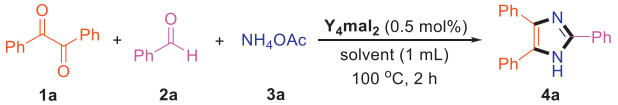

1a 2a 3a 4a

Entry	Solvent	Temperature (°C)	Time (h)	Yield[b] (%)
1[c]	Solvent-free	100	2	15
2	Solvent-free	100	2	69
3	DMC	100	2	53
4	PC	100	2	47
5	H_2O	100	2	0
6	EtOH	100	2	92
7	EtOH	90	2	80
8	EtOH	110	2	98
9	EtOH	110	1.5	89
10	EtOH	110	2.5	97
11[d]	EtOH	110	2	90
12[e]	EtOH	110	2	98

[a] Reaction conditions: benzil (**1a**, 0.2 mmol), benzaldehyde (**2a**, 0.2 mmol), ammonium acetate (**3a**, 0.6 mmol), solvent (1 mL), **Y_4mal$_2$** (0.5 mol%) for 2 h.
[b] The yields were determined by GC with biphenyl as the internal standard.
[c] Without catalyst.
[d] Catalyst loading: 0.4 mol%.
[e] Catalyst loading: 0.6 mol%.

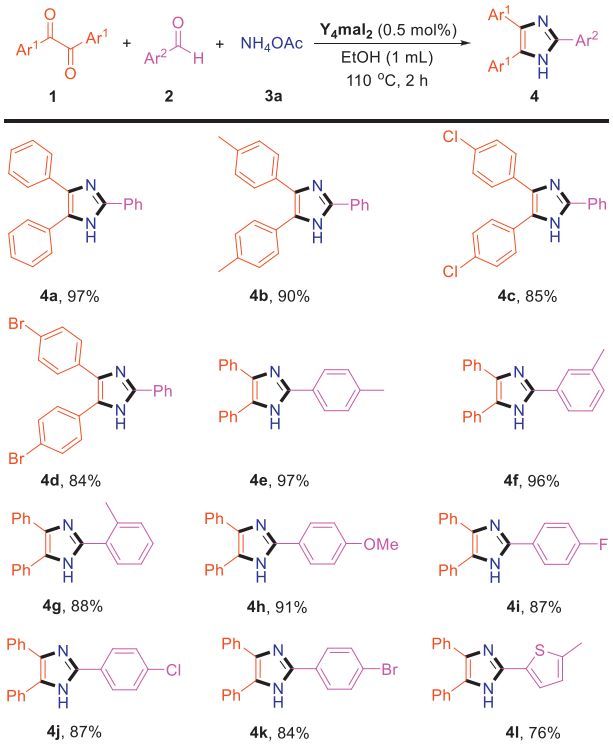

Scheme 1. Scope of benzils and benzaldehydes for imidazole synthesis. Reaction conditions: benzils (**1**, 0.2 mmol), benzaldehydes (**2**, 0.2 mmol), ammonium acetate (**3a**, 0.6 mmol), EtOH (1 mL), **Y_4mal$_2$** (0.5 mol%), 110 °C for 2 h.

To elucidate the compatibility of this catalytic system, various benzils and benzaldehydes were applied for the preparation of 2,4,5-trisubstituted imidazoles under optimal conditions (Scheme 1). A series of 4,4′-disubstituted benzil such as 4,4′-dimethylbenzil, 4,4′-dichlorobenzil, and 4,4′-dibromobenzil could convert into the corresponding imidazoles in good to excellent yield (**4b**-**4d**). Generally, the electron-rich benzils are more dominant for this cyclocondensation transformation. A range of aldehydes containing electron-donating and electron-withdrawing groups were also investigated. Benzaldehydes containing electron-donating groups such as methyl, and methoxy react with benzil and ammonium acetate smoothly, affording corresponding imidazoles with excellent yields (**4e**-**4h**). The cyclocondensation of *p*- and *m*-benzaldehydes proceeded better than *o*-benzaldehyde, indicating the certain effect of steric hindrance. The electron-withdrawing groups such as fluoro, chloro, and bromo on the benzene ring of benzaldehydes were also well tolerated (**4i**-**4k**), but the yields of corresponding imidazoles were lower than that of electron-donating groups. Furthermore, heteroaromatic aldehyde, 5-methylthiophene-2-carbaldehyde was also a good reaction partner, affording the desired product **4l** with 76% yield.

Finally, the practicability of this catalytic system was investigated. Scaling up the model reaction to 5 mmol resulted in a 94% yield of the corresponding imidazole **4a**, indicating the potential of the catalytic system for large-scale production of imidazole derivatives (Fig. 3a). The stability of **Y_4mal$_2$** was verified by FT-IR and PXRD. The characterization spectra of **Y_4mal$_2$** have no obvious

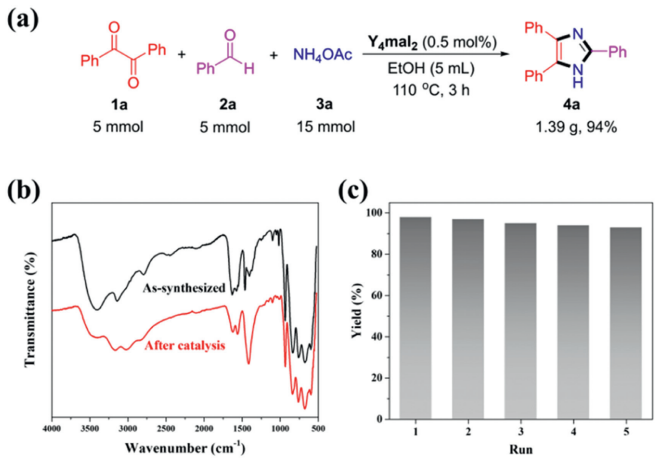

Fig. 3. (a) Gram-scale reaction. (b) The FT-IR spectra. (c) Cycling experiment.

change before and after catalysis, indicating that $\mathbf{Y_4mal_2}$ remains stable in the reaction mixture (Fig. 3b and Fig. S7). The cycling experiment shows that the catalytic performance of $\mathbf{Y_4mal_2}$ without significant decrease after five runs, which further proves the stability of $\mathbf{Y_4mal_2}$ (Fig. 3c).

In summary, we successfully synthesized a rare racemic Y(III)-containing antimonotungstate dimer by one-pot method from an aqueous solution. The resulting polyanion exhibits a fascinating asymmetric handshake-like configuration induced by the chiral configuration of D- or L-mal ligands. Notably, $\mathbf{Y_4mal_2}$ demonstrates remarkable Lewis acid catalytic activity and good stability in the cyclocondensation of aldehydes, benzil, and ammonium acetate. This environmentally friendly approach allows for the efficient synthesis of substituted 2,4,5-triarylimidazoles in good to excellent yields using EtOH as a green solvent under mild reaction conditions. This work represents the application of RE-POMs in the field of catalysis, potentially opening up new avenues for the synthesis of heterocyclic compounds. Further investigations into the structural and catalytic properties of RE-POMs are currently underway.

Declaration of competing interest

The authors declare that they have no known competing financial interests or personal relationships that could have appeared to influence the work reported in this paper.

CRediT authorship contribution statement

Guoping Yang: Writing – review & editing, Resources, Project administration, Methodology, Funding acquisition, Conceptualization. **Zhoufu Lin:** Investigation, Data curation. **Xize Zhang:** Investigation. **Jiawei Cao:** Investigation, Data curation. **Xuejiao Chen:** Investigation. **Yufeng Liu:** Writing – original draft, Methodology, Funding acquisition. **Xiaoling Lin:** Validation, Investigation, Formal analysis. **Ke Li:** Writing – original draft, Methodology, Investigation, Funding acquisition, Formal analysis.

Acknowledgments

This work was supported by the National Natural Science Foundation of China (Nos. 22301034, 22301033) and the Jiangxi Provincial Natural Science Foundation (No. 20232ACB213005).

Supplementary materials

Supplementary material associated with this article can be found, in the online version, at doi:10.1016/j.cclet.2024.110274.

References

[1] J.J. Berzelius, Ann. Phy. 82 (1826) 369–392.
[2] M. Wang, J.Y. Pang, J.P. Wang, J.Y. Niu, Coord. Chem. Rev. 508 (2024) 215730.
[3] S.R. Li, Z.Z. Weng, L.P. Jiang, et al., Chin. Chem. Lett. 34 (2023) 107251.
[4] G.P. Yang, K. Li, C.W. Hu, Inorg. Chem. Front. 9 (2022) 5408–5433.
[5] R. Huang, W.W. Wang, C. Zhang, et al., Chin. Chem. Lett. 33 (2022) 3955–3960.
[6] Y.F. Liu, G.D. Zeng, Y.T. Cheng, et al., Chin. Chem. Lett. 35 (2024) 108480.
[7] Y.F. Liu, C.W. Hu, G.P. Yang, Chin. Chem. Lett. 34 (2023) 108097.
[8] Z.Y. Liu, Y.D. Lin, H.N. Chen, et al., Tungsten 4 (2022) 81–98.
[9] M.Z. Chi, Y. Zeng, Z.L. Lang, et al., ACS Catal. 14 (2024) 5006–5015.
[10] Q.L. Hu, K. Li, X.J. Chen, Y.F. Liu, G.P. Yang, Polyoxometalates 3 (2024) 9140048.
[11] X.Y. Liu, Y.H. Yu, Y.F. Sun, W.H. Fang, J. Zhang, Polyoxometalates 2 (2023) 9140045.
[12] S.S. Wang, G.Y. Yang, Chem. Rev. 115 (2015) 4893–4962.
[13] Y. Cheng, K.J. Qin, D.J. Zang, Rare Met. 42 (2023) 3570–3600.
[14] L.L. Liu, L. Wang, X.Y. Xiao, et al., Coord. Chem. Rev. 506 (2024) 215687.
[15] V. Das, R. Kaushik, F. Hussain, Coord. Chem. Rev. 413 (2020) 213271.
[16] M. Nyman, P.C. Burns, Chem. Soc. Rev. 41 (2012) 7354–7367.
[17] C. Boskovic, Acc. Chem. Res. 50 (2017) 2205–2214.
[18] Y.F. Liu, Q.L. Hu, X.J. Chen, et al., Rare Met. 43 (2024) 1316–1322.
[19] Q.Y. Hu, H.S. Zhou, Y. Ding, T. Wågberg, X.B. Han, ACS Catal. 14 (2024) 5898–5910.
[20] Q.Y. Hu, S.S. Chen, T. Wågberg, et al., Angew. Chem. Int. Ed. 62 (2023) e202303290.
[21] X.B. Han, Y.G. Li, Z.M. Zhang, et al., J. Am. Chem. Soc. 137 (2015) 5486–5493.
[22] Z.C. Zhao, M.Y. Zhao, L. Deng, et al., Chem. Commun. 60 (2024) 5415–5418.
[23] Y.Q. Feng, F.Y. Fu, L.L. Zeng, et al., Angew. Chem. Int. Ed. 63 (2024) e202317341.
[24] J. Zhang, Y.Y. Dong, L. Deng, et al., Nanoscale 16 (2024) 11518–11523.
[25] Q. Li, F.Y. Fu, M.Y. Zhao, et al., Chin. Chem. Lett. (2024), doi:10.1016/j.cclet.2024.110090.
[26] X.K. Fang, T.M. Anderson, Y. Hou, C.L. Hill, Chem. Commun. 40 (2005) 5044–5046.
[27] M.N. Sokolov, N.V. Izarova, E.V. Peresypkina, D.A. Mainichev, V.P. Fedin, Inorg. Chim. Acta 362 (2009) 3756–3762.
[28] P.T. Ma, R. Wan, Y.A. Si, et al., Dalton Trans. 44 (2015) 11514–11523.
[29] P.T. Ma, Y.Y. Wang, Y.A. Si, J.P. Wang, J.Y. Niu, Inorg. Chem. Commun. 83 (2017) 84–87.
[30] H.C. Wu, R. Wan, Y.A. Si, et al., Dalton Trans. 47 (2018) 1958–1965.
[31] Y.L. Wang, J.W. Zhao, Z. Zhang, et al., Inorg. Chem. 58 (2019) 4657–4664.
[32] H.H. Chen, L. Sun, J.P. Zhang, et al., Dalton Trans. 49 (2020) 12458–12465.
[33] S.S. Xie, D. Wang, Z.X. Wang, et al., Inorg. Chem. Front. 9 (2022) 350–362.
[34] B.X. Niu, Y.Z. Song, A.Q. Yu, et al., Inorg. Chem. 63 (2024) 8791–8798.
[35] P.T. Ma, F. Hu, Y. Huo, et al., Cryst. Growth Des. 17 (2017) 1947–1956.
[36] D. Wu, W.L. Chen, T. Wang, et al., Dyes Pigments 168 (2019) 151–159.
[37] E. Tanuhadi, N.I. Gumerova, A. Prado-Roller, A. Mautner, A. Rompel, Inorg. Chem. 60 (2021) 8917–8923.
[38] I. Ali, M.N. Lone, H.Y. Aboul-Enein, Med. Chem. Commun. 8 (2017) 1742–1773.
[39] A.M. Vijesh, A.M. Isloor, S. Telkar, et al., Eur. J. Med. Chem. 46 (2011) 3531–3536.
[40] S. Kankala, R.K. Kankala, P. Gundepaka, et al., Bioorg. Med. Chem. Lett. 23 (2013) 1306–1309.
[41] M.A. Zolfigol, S. Baghery, A.R. Moosavi-Zare, S.M. Vahdat, RSC Adv. 5 (2015) 32933–32940.
[42] D. Kumar, D.N. Kommi, N. Bollineni, A.R. Patel, A.K. Chakraborti, Green Chem. 14 (2012) 2038–2049.
[43] A. Shaabani, R. Afshari, S.E. Hooshmand, M.K. Nejad, ACS Sustain. Chem. Eng. 5 (2017) 9506–9516.
[44] M. Masteri-Farahani, A. Ezabadi, R. Mazarei, et al., Appl. Organomet. Chem. 34 (2020) e5727.
[45] M. Esmaeilpour, J. Javidi, M. Zandi, New J. Chem. 39 (2015) 3388–3398.
[46] M.S. Raghu, C.B. Pradeep Kumar, K.N.N. Prasad, et al., ACS Comb. Sci. 22 (2020) 509–518.
[47] J. Jayram, V. Jeena, Green Chem. 19 (2017) 5841–5845.
[48] K. Li, Y. Liu, G. Yang, et al., Green Chem. 26 (2024) 6454–6460.
[49] Q.L. Hu, Y.F. Liu, X.L. Lin, et al., Inorg. Chem. 63 (2024) 8919–8924.
[50] Y.F. Liu, X.L. Lin, B.M. Ming, et al., Inorg. Chem. 63 (2024) 5681–5688.
[51] J.H. Ding, Y.F. Liu, Z.T. Tian, et al., Inorg. Chem. Front. 10 (2023) 3195–3201.
[52] K. Li, Y.F. Liu, X.L. Lin, G.P. Yang, Inorg. Chem. 61 (2022) 6934–6942.